Applied Energy 261 (2020) 114360

Contents lists available at ScienceDirect

Applied Energy

journal homepage: www.elsevier.com/locate/apenergy

Optimizing the operation of energy storage using a non-linear lithium-ion battery degradation model

Arpit Maheshwari[a,b], Nikolaos G. Paterakis[a,*], Massimo Santarelli[b], Madeleine Gibescu[c]

[a] Department of Electrical Engineering, Eindhoven University of Technology, 5600MB Eindhoven, the Netherlands
[b] Politecnico di Torino, Corso Duca Degli Abruzzi 24, 10129 Turin, Italy
[c] Copernicus Institute of Sustainable Development, Utrecht University, 3584CB Utrecht, the Netherlands

HIGHLIGHTS

- A degradation-aware market participation model for stationary storage is proposed.
- A non-linear degradation model is built from experimental data for Li-ion batteries.
- The non-linear degradation model is compatible with a MILP formulation.
- A decomposition technique for solving efficiently long-horizon problems is proposed.
- The proposed model is benchmarked against commonly used degradation models.

ARTICLE INFO

Keywords:
Lithium-ion batteries
Energy markets
Degradation
Cycle aging
Optimization

ABSTRACT

Given their technological and market maturity, lithium-ion batteries are increasingly being considered and used in grid applications to provide a host of services such as frequency regulation, peak shaving, etc. Charging and discharging these batteries causes degradation in their performance. Lack of data on degradation processes combined with requirement of fast computation have led to over-simplified models of battery degradation. In this work, the recent experimental evidence that demonstrates that degradation in lithium-ion batteries is non-linearly dependent on the operating conditions is incorporated. Experimental aging data of a commercial battery have been used to develop a scheduling model applicable to the time constraints of a market model. A decomposition technique that enables the developed model to give near-optimal results for longer time horizons is also proposed.

1. Introduction

Lithium-ion battery technology has increased in popularity in recent years driven by its demand in electric vehicles [1,2]. The combination of performance, flexibility and decreasing costs has also made it attractive for integration in power systems. Numerous studies shed light upon scheduling strategies for battery-based storage in providing grid services. However, lithium-ion batteries have a limited life [3–5]. With time and use degradation processes occur, leading to a loss in capacity (capacity fade) and a loss in power capability (power fade). Thus, accurate determination of degradation is imperative in such models, not only in order to be realistic in determining the business case, but also to develop intelligent strategies for charge–discharge scheduling of these batteries.

1.1. Literature review

Several market studies on batteries focus on the economic viability of the storage options from a long-term perspective, while others focus on optimizing their short-term operational strategy. The modus operandi of such studies is to develop a model that jointly simulates the market and battery behaviour. Modelling of the market mechanisms has been comprehensive, with studies considering a single [6,7], multiple [8,9] or a combination of markets [10–12], assuming perfect price information [8,9,13,14] or uncertainty in prices [12,15].

Battery models in power system and market studies often completely ignore degradation [13,15,16]. In some works, degradation is calculated post-optimization. As a result, the operation strategy is short-sighted and does not consider the battery as a time-limited and costly resource [17–20].

* Corresponding author.
E-mail address: n.paterakis@tue.nl (N.G. Paterakis).

https://doi.org/10.1016/j.apenergy.2019.114360
Received 22 October 2019; Received in revised form 26 November 2019; Accepted 10 December 2019
Available online 30 December 2019

Nomenclature

Parameters

l	parameter representing the horizontal change between two consecutive points defining the piecewise linear function δ^{1C}
m	parameter representing the vertical change between two consecutive points defining the piecewise linear function δ^{1C}
n	total number of segments of a piecewise linear function
s	parameter representing SOC values of points defining the piecewise linear function δ^{1C}
I_{1C}	1C current (A)
$P_t^{ch,max}$	maximum power input to the battery in the trading interval t (W)
$P_t^{dis,max}$	maximum power output from the battery in the trading interval t (W)
Q	rated capacity of the battery (Ah)
V_{nom}	nominal battery voltage (V)
$\delta^{1C}(s)$	parameter representing y coordinates of points defining the piecewise linear function δ^{1C}
η	efficiency of the storage system
λ_t	market clearing price for the trading interval t (€/ Wh)
ω	weighting factor
ΔT	duration of a trading interval (h)

Decision Variables

d_t	degradation during the trading interval t (Ah)
d_t^{1C}	degradation at 1C current rate for the change in battery state during the trading interval t (Ah)
i_t	current rate during the trading interval t (h^{-1})
u_t	binary variable. 1 when storage system is charging in trading interval . else 0
$v_{t,i}$	modelling variable introduced to implement incremental cost formulation
$z_{t,i}$	binary variable introduced to implement incremental cost formulation
D	total degradation in the market period (Ah)
$P_t^{ch,b}$	power input to the battery in the trading interval t (W)
$P_t^{ch,m}$	power input from the market in the trading interval t (W)
$P_t^{dis,b}$	power output from the battery in the trading interval t (W)
$P_t^{dis,m}$	power output to the market in the trading interval t (W)
R	revenue (€)
SOC	state of charge, measure of the remaining capacity of the battery, defined as the ratio of the current capacity to the total capacity, expressed in percent
δ_t^{1C}	cumulative degradation function value computed for 1C at the end of trading interval t
ζ	composite objective function value
ψ	degradation scaling factor to account for current dependence

Indices

i	index of points defining the piecewise linear function
t	trading interval index

Terms

DOD	depth of discharge or cycle depth, defined as one half of the fraction of full cell capacity used during one cycle, expressed in percent
EFC	equivalent full cycle, a measure of charge throughput equal to two times the capacity of a new battery
SOC_t	state of charge of the storage system at the end of trading interval t

Degradation-aware battery scheduling studies use either a constraint-based approach [11,21,12] or an objective-based approach [9,22,23]. In [10], the constraint-based approach has even been combined with the objective-based approach. In the constraint-based approach, to extend the life of the battery, one or more of the following variables are constrained: power, number of cycles per day, depth of discharge (DOD), maximum and minimum state of charge (SOC). Such approaches that do not model the degradation behaviour at all return non-optimal results.

In the objective-based approach, the cost of battery degradation is included as an economic cost in the objective function. Traditionally two main methods to model degradation have been used: the Ah throughput method [23,24] and the method of cycle life vs. DOD power function [9,11,22]. In the first method, it is assumed that a certain amount of energy can be cycled through a battery before its end of life, irrespective of the depth of discharge. In the second method it is assumed that the number of cycles that a battery can perform is inversely proportional to the amplitude of DOD given by a simple power function. The origins of the two most employed methods for quantifying degradation, cycle life vs. DOD and Ah throughput, can be traced to modelling the lead-acid battery degradation behaviour [25–27].

From the point of view of objective function, most approaches are single objective, where degradation is assigned an economic cost. This cost is often based on the battery replacement cost [9,18,28,29], sometimes on the economic utilization costs (investment & operating) [30] and other times on the marginal cost of operation [31]. The above discussion has been summarized in Fig. 1.

1.2. Gaps in modelling degradation phenomena in lithium-ion batteries

While the modelling of the market part of the scheduling models has been comprehensive, modelling of battery degradation phenomena is

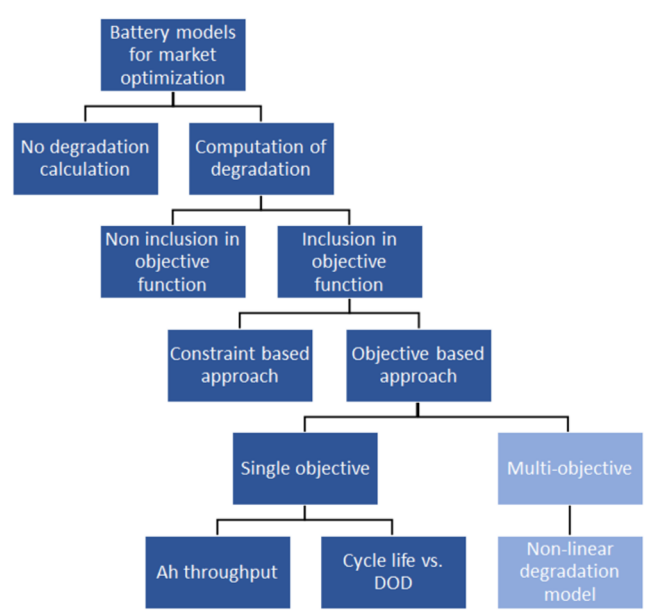

Fig. 1. Summary of battery models used for market studies (the contribution of this work highlighted using a lighter shade).

inadequate in market-based scheduling models for lithium-ion batteries because of either the high complexity and subsequent computational burden associated with some non-linear models [32] or due to completely ignoring the effects of current and SOC on degradation in very simple models. The reasons for this are partly paucity of data for developing detailed models and partly the requirement for such models to be simple and computationally effective. The former arises from the fact that aging in batteries is not completely understood and is a subject of ongoing research, while the latter stems from the practical constraint of being able to optimize within the time horizons of market trading when using the computational power that is currently available and algorithmic know-how.

Neither the DOD vs. cycle life method nor the Ah throughput method consider the dependence on current or SOC. In Section 2 of this study, it is shown why these methods are inadequate in representing the aging behaviour in lithium-ion batteries used in this work.

1.3. Contribution

Having recognized the gaps in modelling degradation phenomena in lithium-ion batteries for optimization studies, the contribution of this work is threefold:

- A market-based lithium-ion battery scheduling model that considers the effect of both the current and the state of charge on degradation of lithium-ion batteries in order to optimize short-term operations is developed. The degradation data come from long-duration experimental studies of a commercial lithium-ion battery. Since the degradation behaviour is non-linear, the optimality of the scheduling strategy is ensured by casting the model as a mixed-integer linear program (MILP). It is to be noted that the proposed model has been developed for stationary storage applications. For this reason the effect of temperature on degradation has not been considered because battery modules are placed in temperature regulated containers.
- A multi-objective approach where revenue and degradation are treated as separate objectives is introduced, putting the onus on a (human) decision maker on choosing the desired scheduling strategy. This approach is more transparent and flexible in a dynamic market situation. Moreover, no artificial constraints except for limiting the maximum input/output power are considered in the model. The upper limit is based on the availability of experimental data for the batteries under consideration.
- The proposed model that captures non-linearity in battery degradation behaviour in a multi-objective optimization problem setting is more realistic and accurate but also more complex. A two-stage temporal decomposition technique that allows more trading intervals to be handled but still returns near-optimal scheduling strategies in a limited computation time is proposed and demonstrated.

The remainder of this paper is organized as follows: first, deficiencies of traditional degradation modelling based on recent experimental evidence are elucidated in Section 2. Then, a scheduling model that takes into account the non-linearities in lithium-ion battery degradation behaviour is proposed in Section 3. In order to solve computationally intensive optimization problems, a two-stage temporal decomposition technique is introduced in Section 4. The results of a case study considering a day-ahead market where the benefits of the current approach are shown and the degradation calculation is compared against other established approaches are presented in Section 5. It is to be noted that the choice of the day-ahead market in the case study is incidental to this work. Application of the decomposition technique to a week-long market horizon is also demonstrated in this section. Finally, the paper is concluded in Section 6.

2. Nature of aging in lithium-ion batteries

The capacity of a battery over time is not constant. The main factors that cause decline in the capacity can be divided into:

- External factors: temperature, time
- Internal factors: SOC, current, DOD

2.1. Calendar and Cycle aging

Aging processes are often studied separately as calendar and cycle aging. Calendar aging refers to degradation in battery performance during storage (no load conditions), while cycle aging refers to degradation while charging and discharging the batteries. Capacity is the leading health indicator of the battery. When the capacity of a battery is about 70–80% of the original capacity, it is usually retired from its primary application. In this work, degradation refers to the loss of capacity that a battery experiences. This work is a short-term study where the operational strategy of a battery is optimised. Thus, only cycle aging is considered in the degradation model. Moreover, for the batteries under study, pure calendar aging is quite low in comparison with the cycle aging [33]. In addition to that, the temperature is assumed to be regulated through a heat management system, an essential component of energy storage systems. All values of degradation parameters used in this work were determined for 20°C. Hence, in this work, optimization is carried out considering only the internal factors.

2.2. Dependance on internal factors

The characteristics of the lithium-ion battery considered in this work are listed in Table 1. This battery was extensively characterized to analyze cycle aging in [34].

The invalidity of the cycle life vs. DOD method is evident when the aging behaviour of the battery is plotted for two tests that were conducted at the same temperature, current and DOD as seen in Fig. 2a. The only difference between the tests is the average state of charge around which the cells are cycled. The number of equivalent full cycles (equivalent to the Ah throughput, where one EFC = 4.3 Ah for this battery) until a capacity of 80% is substantially lower in the test case where cells where cycled around SOC = 50% than around SOC = 25%. Similar results are reported in [35–37], where it is observed that depth of the cycle needs to be considered along with the mean SOC in order to analyse degradation, while in [38] a physical model to explain the effect of mean SOC has been developed. This behaviour has been assigned to the volume changes in the graphite electrode present in most lithium-ion batteries. Not only the cycle life vs. DOD but also the Ah throughput method does not consider this effect of average SOC on battery degradation.

In Fig. 2b the effect of current on capacity fade is depicted. The number of equivalent full cycles until the cell capacity decreases to 80% is considerably different for the two currents shown. Evidently, the effect of current in the degradation models used in battery scheduling strategies cannot be ignored.

Table 1
Battery properties for this case study.[1]

Property	Value
Chemistry	Nickel Manganese Cobalt (NMC)
Type	18650
Rated Capacity (Ah)	2.15
Nominal Voltage (V)	3.7
1C current (A)	2.15
Cycle performance at 5A discharge	88% of initial capacity at 500 cycles

[1] Data from manufacturer Sony Energy Devices Corporation, Model Number US18650V3.

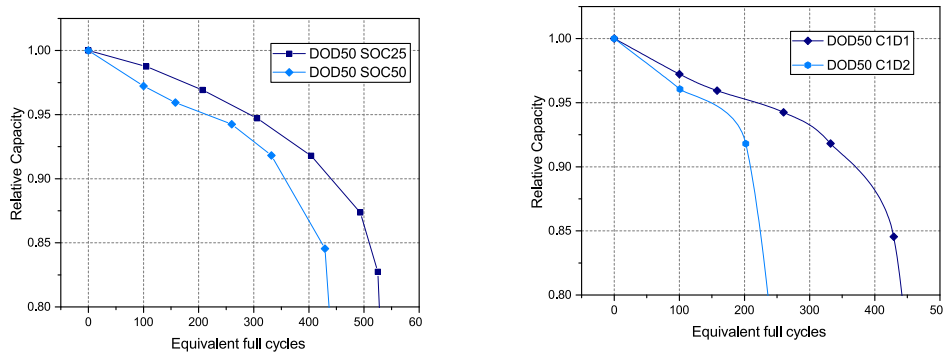

(a) Different average SOC cases.

(b) Different current case, C refers to charging rate, D refers to discharging rate.

Fig. 2. Experimental aging behaviour in the NMC batteries [34].

2.3. Quantification of degradation

As discussed in the previous section, the study of battery cycle life as a function of DOD has little significance without considering the effect of SOC. In [34], the combined effect of SOC and DOD on battery aging was quantified in terms of degradation parameters. They are shown for 1C current in Fig. 3a. The effect of current rate was found to be independent of the effect of SOC and DOD. Parameters for 2C current were found to be a constant 30% higher than the parameters at 1C current.

From Fig. 3a, areas of high degradation can be observed at high and low SOC. Low degradation is observed in the SOC range from 30% to 60%. This is a common observation in lithium-ion battery testing [35,36] and as described before, it does not fit with the traditional cycle life vs. DOD and Ah throughput models. To visualize the non-linear nature of aging for these batteries, degradation in terms of capacity fade for every possible change of state of the battery is mapped in Fig. 3b. The surface has been shown for the two current rates that were experimentally tested. The graph is symmetric along the $x = y$ plane, which means that degradation is direction-independent and depends only on the initial and final SOC. However, it is path-dependent and non-linear. The transition states that cause lower or higher degradation can be more easily observed by referring to the contour map displayed in Fig. 3c.

3. Multi-objective scheduling model

The proposed model is distinguished from existing models on two main counts. First is how the degradation is handled given the non-linearity and second on how the degradation is treated as a second objective along with revenue from market trading.

The composite objective function to be maximized is given by (1), where ζ is a free fictitious variable.

$$\zeta = \omega \cdot R - (1 - \omega) \cdot D \tag{1}$$

The values of revenue R and degradation D are scaled in order to be of the same order of magnitude. The weighting factor ω is varied between 0 and 1 in a parametric sweep to generate Pareto optimal scheduling strategies. The two objective functions are detailed in (2) and (3).

$$R = \sum_t [\lambda_t \cdot (P_t^{dis,m} - P_t^{ch,m})] \cdot \Delta T \quad \forall\, t \tag{2}$$

In (2) λ_t is the market clearing price, assumed to be a known parameter for the optimization. In this study, a single energy market is considered. However, multiple markets can be considered in a fashion similar to the one described in [39]. It is to be noted that the proposed model can be readily embedded in other applications by simply replacing the objective function, e.g., with the maximization of privacy or self-consumption.

The total battery degradation during the entire duration of the decision making horizon can be calculated by adding together the degradation incurred during each time interval (d_t) as defined by (3).

$$D = \sum_t d_t \quad \forall\, t \tag{3}$$

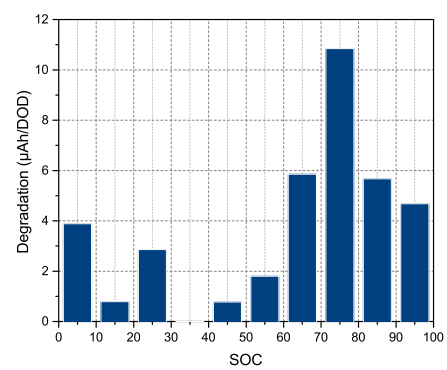

(a) 1C rate degradation parameters determined from experiments

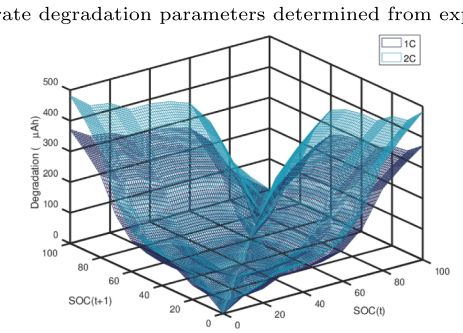

(b) Mapped degradation surface for 1C and 2C rates

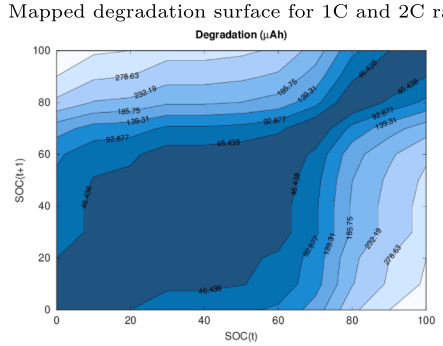

(c) Contour map of degradation for 1C rate

Fig. 3. Degradation behaviour of lithium-ion batteries.

The SOC of the battery is updated by (4) depending on whether charging or discharging takes place during a time interval.

$$SOC_t = SOC_{t-1} + \frac{(P_t^{ch,b} - P_t^{dis,b})\cdot\Delta T}{V_{nom}\cdot I_{1C}} \quad \forall\, t > 1 \tag{4}$$

The lower bound of zero and the upper bound on the power capability of the battery are set through (5) and (6). Using the binary variable u_t, it also ensures that during any trading interval, the storage system either charges or discharges.

$$0 \leqslant P_t^{ch,b} \leqslant P^{ch,max}\cdot u_t \quad \forall\, t \tag{5}$$

$$0 \leqslant P_t^{dis,b} \leqslant P^{dis,max}\cdot(1 - u_t) \quad \forall\, t \tag{6}$$

The process of energy conversion in the storage system is not 100% efficient, a fact that is taken into account by (7) and (8). These equations distinguish the battery input/output power (subscript b) from that exchanged in the market (subscript m). An efficiency factor η is assigned to the conversion and transmission processes. In reality, η is not a constant but it is also a factor of operating and environmental conditions. If this is factored in, it will introduce additional non-linearity and complexity in the proposed model. However, given the overall high efficiencies of lithium-ion batteries, it has been assumed a constant in this work.

$$P_t^{ch,b} = P_t^{ch,m}\cdot\eta \quad \forall\, t \tag{7}$$

$$P_t^{dis,b}\cdot\eta = P_t^{dis,m} \quad \forall\, t \tag{8}$$

The SOC of the battery (given in percentage) is constrained by (9) because of its definition.

$$0 \leqslant SOC_t \leqslant 100 \quad \forall\, t \tag{9}$$

Observing that higher currents lead to greater degradation in batteries, the degradation for every market time interval is expressed in a bilinear form in (10) with the degradation at 1C as a basis. The equation relates the actual degradation caused in the battery in a time interval (d_t) to the degradation that will be caused in the battery for the same change of state but at 1C current rate (d_t^{1C}). It introduces through the scaling factor Ψ the non-linearity caused by the effect of current on degradation. Ψ is a function of the current rate i_t which is calculated in (11). In this equation, the current rate has been determined using a constant value of voltage (nominal battery voltage, V_{nom}). In reality, however, the voltage of the battery is not constant but a function of the state of charge. Including this dependency is outside the scope of this work as it will lead to additional non-linearity and computational burden.

$$d_t = d_t^{1C}\cdot\Psi_t \quad \forall\, t \tag{10}$$

The above equation relates the degradation happening in any time interval to both SOC and current rate. The SOC dependence is given by d_t^{1C} and has been mapped beforehand based on experimental data as shown in Fig. 3c. The influence of current on degradation is given by Ψ_t which is explained below.

$$i_t = \frac{(P_t^{ch,b} + P_t^{dis,b})}{V_{nom}\cdot I_{1C}} \quad \forall\, t \tag{11}$$

This scaling factor Ψ is equal to zero at no load conditions (0C) as no cycle aging takes place when the battery is idle. Being based on 1C current rate, it has the value of 1 at 1C. From the experimental data in [34], its value at 2C is determined to be 1.2956. Since intermediate experiments at other current values were not carried out, it has been assumed that the parameters scale linearly between 0C - 1C and 1C - 2C. For example, if the current rate is 1.5C, the scaling factor is the average of 1 and 1.2956.

Assuming a linear scaling factor in the absence of more precise data for intermediate current values can be a reasonable assumption because increasing current causes increasing degradation in the battery. Thus, the scaling factor will be a monotonically increasing function of current. Accuracy can be improved by adding the intermediate values of the scaling factor if experimental results for more current values are available. This can be achieved without any change in the structure of the developed model.

In order to determine d_t^{1C} for each change in battery state, the experimental data on degradation at 1C current rate is first expressed in a cumulative form as shown in Fig. 4. The cumulative degradation function is made up of n segments (in this case $n = 10$). This cumulative degradation function (δ_t^{1C}) does not have a physical significance unlike d_t^{1C}. It is a mathematical tool, conceived in order to implement the non-linear degradation behaviour represented in Fig. 3, in the framework of MILP. Using the cumulative function facilitates modelling as degradation during a time interval (d_t^{1C}) can be simply determined as a difference of the cumulative degradation values before and after the trading interval. This is expressed in (12).

$$d_t^{1C} = |\delta_t^{1C} - \delta_{t-1}^{1C}| \quad \forall\, t \tag{12}$$

The value of δ_t^{1C} is determined using the incremental cost formulation [40,41]. This formulation allows accessing a piecewise linear function such as the one of Fig. 4 in a MILP. To implement the incremental cost formulation at any time interval t, the piecewise linear cumulative degradation function of Fig. 4 is specified by the points $(s_{t,i}, \delta^{1C}(s_{t,i}))\ \forall\, i \in \{0,...,n\}$ where n is the total number of segments. Thus, $s_{t,i}$ is the x-coordinate and $\delta^{1C}(s_{t,i})$ is the y-coordinate of the points highlighted in Fig. 4.

Next let, $l_{t,i} = s_{t,i} - s_{t,i-1}$ and $m_{t,i} = \delta^{1C}(s_{t,i}) - \delta^{1C}(s_{t,i-1})\ \forall$ i.

Any value of the state of charge SOC_t such that $s_{t,0} \leqslant SOC_t \leqslant s_{t,n}$ can be written as in (13).

$$SOC_t = s_{t,0} + \sum_{i=1}^{n} v_{t,i} \tag{13}$$

The introduced variable $v_{t,i}$ is bounded $0 \leqslant v_{t,i} \leqslant l_{t,i}\ \forall$ i.

Then the cumulative degradation function value for time interval t and SOC_t is given by (14).

$$\delta_t^{1C} = \delta_t^{1C}(s_0) + \sum_{i=1}^{n} \frac{m_{t,i}}{l_{t,i}}\cdot v_{t,i} \tag{14}$$

if $v_{t,i} < l_{t,i}$, $v_{t,i+1} = 0\ \forall\, i \in \{1,...,n-1\}$ holds true.

This can be enforced in the MILP through constraints (15)–(17) in which the binary variables $z_{t,i}$, $i \in \{1,...,n-1\}$ are introduced.

$$l_{t,1}\cdot z_{t,1} \leqslant v_{t,1} \leqslant l_{t,1} \tag{15}$$

$$l_{t,i}\cdot z_{t,i} \leqslant v_{t,i} \leqslant l_{t,i-1}\cdot z_{t,i-1}\ \forall\, i \in \{2,...,n-1\} \tag{16}$$

$$0 \leqslant v_{t,i} \leqslant l_{t,i}\cdot z_{t,n-1} \tag{17}$$

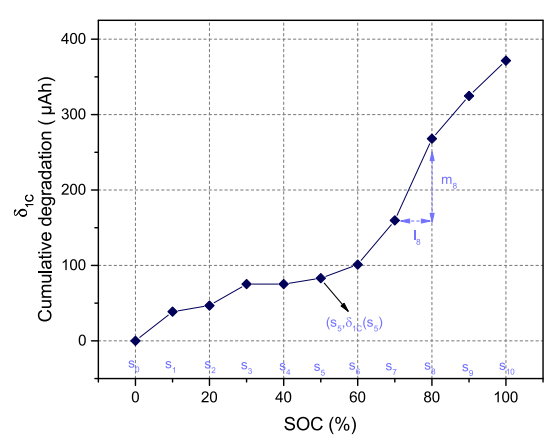

Fig. 4. Cumulative degradation function. Annotations to clarify the implementation of the incremental cost formulation (13)–(17) are shown in a lighter shade of blue.

The product of d_t^{1C} and Ψ_t which gives the actual degradation d_t is calculated using the identity (18).

$$d_t^{1C}\cdot\Psi_t = \left(\frac{d_t^{1C}+\Psi_t}{2}\right)^2 - \left(\frac{d_t^{1C}-\Psi_t}{2}\right)^2 \tag{18}$$

These two squares are approximated by piecewise linear formulations. To determine the values of the square as well as Ψ_t from their piecewise linear functions, an incremental cost formulation is used, similar to the implementation in (13)–(17). This method introduces $n-1$ binaries and $2n$ constraints where n is the number of segments of the piecewise linear function. The absolute value in (12) is determined by adding inequalities (19) and (20) to the model.

$$|\delta_t^{1C} - \delta_{t-1}^{1C}| \geqslant \delta_t^{1C} - \delta_{t-1}^{1C} \tag{19}$$

$$|\delta_t^{1C} - \delta_{t-1}^{1C}| \geqslant \delta_{t-1}^{1C} - \delta_t^{1C} \tag{20}$$

Given the nature of the optimization, where degradation is penalized, this formulation using the two inequalities computes the absolute value of δ_t^{1C}-δ_{t-1}^{1C} which is equal to d_t^{1C}.

To summarize the developed model, Eqs. (1)–(3) define the objective functions. (1) is tied to (2) and (3) through the weighting factor ω. (4) updates the state of the battery after every market trading interval. (5) and (6) are constraints that limit the maximum power input and output and also ensure that battery is either charged or discharged in any time interval. (7) and (8) account for inefficiencies in battery systems. (9) sets the boundaries on the state of charge. (10)–(12) together calculate the degradation in any time interval. Eqs. (13)–(20) convert the non-linear problem into a MILP by introducing extra constants (s, l, m, $\delta^{1C}(s)$), continuous variables (v), binary variables (z), identity (18) and inequalities (19) and (20). Eqs. (13)–(17) describe the incremental cost formulation to account for piecewise linear functions, (18) suggests the way to deal with bilinear terms while the inequalities of (19) and (20) solve the problem of calculating the modulus function exploiting the problem setup.

4. Two-stage decomposition technique

A scheduling algorithm is only useful when it can generate an optimal strategy (or at least a near-optimal strategy) within computational time restrictions imposed by the market horizon. For cases where greater accuracy is desired (e.g. by increasing the linear segments defining a non-linear function) or when optimizing for more trading intervals such as for multiple days in the day-ahead market or for the imbalance market (for example with 15-min trading intervals), the optimization routine might be unable to provide solutions with near-zero optimality gap within reasonable time. In this section, a decomposition technique is developed to enable computation for these cases while delivering near-optimal solutions much quicker than the original program.

The decomposition method works by breaking the problem in the time domain into smaller tractable sub-problems. By tractable, it is implied that each of these sub-problems can be solved with a zero optimality gap in a reasonable time-frame with the computing resources at hand. By examining the structure of the optimization problem, the block variable d_t^{1C} is computed as the difference of two consecutive time interval values of δ^{1C} where δ^{1C} is only a function of SOC (complicating constraints). Thus, fixing an intermediate SOC value, effectively divides the problem into two independent sub-problems.

Fixing the intermediate SOC at 50% is a good heuristic as it hedges equally on the possibility of both charging and discharging. However, an even better guess for setting the intermediate SOC is possible. This is achieved by solving the original (non-decomposed) optimization problem for the entire market horizon for a fixed period of computation time or optimality gap, whichever comes earlier. The best feasible solution at this stage is used for fixing the intermediate SOC values. Typically, a commercial solver (such as CPLEX) finds good feasible solutions in little time initially but then has difficulty in closing the optimality gap. These SOC values provide a better initial guess than fixing the intermediate SOC state at 50%. Thereafter, the decoupled sub-periods are solved individually. The two-stage methodology is graphically shown in Fig. 5. It is to be noted that decomposition in the time domain has been applied to other optimization problems as well [42].

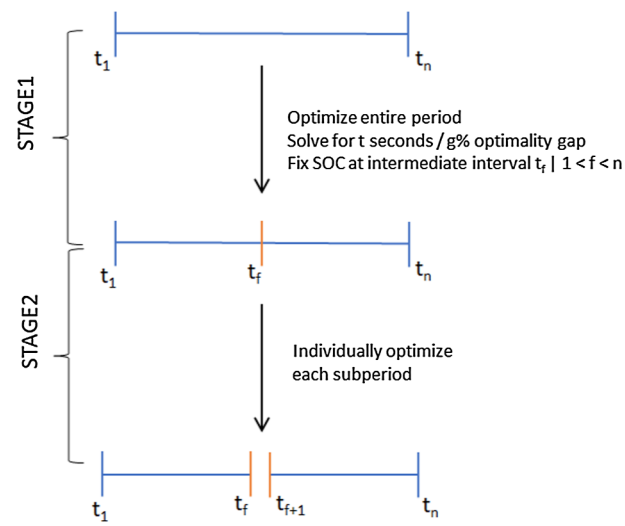

Fig. 5. Illustration of the two-stage temporal decomposition method.

5. Numerical Case Study

The proposed model is implemented using GAMS 24.8.5 and the MILP problem is solved using CPLEX 12. In order to demonstrate the functioning, results and advantages of the model compared to contemporary approaches, the application of the lithium-ion battery in a day-ahead market setup is investigated in this case study. A 1MWh / 2MW storage system is considered for the case study the basic unit of which is made of the commercial cell of Table 1. It is assumed that the storage system is controlled by a battery management system that ensures that the cells of the storage system are at the same state at all times. The one-way efficiency of this system (η) is assumed to be 95%. The day-ahead market prices on Monday, 22 January 2018 for the UK SEM were obtained from ENTSO-E online platform [43]. This day-ahead market has half-hourly trading intervals ($\Delta T = 0.5$). It is assumed that the storage system acts as a price-taker. It is reiterated that this study focuses on an efficient scheduling of the storage system and not on the economics of the application of storage in different markets or their combinations. The choice of this particular market is motivated not from an economic perspective but because it fits the charge–-discharge characteristics of the battery under study and therefore, facilitates illustrating the usability of the proposed degradation model in a didactic fashion.

5.1. Revenue maximization

First, optimization is carried out with the *naive* objective of solely maximizing revenue. Degradation is computed but it does not affect the scheduling strategy, which is geared towards extracting the maximum financial gain possible from the day-ahead market. This case is considered the base case against which multi-objective scheduling strategies can be compared. Note that this case corresponds to $\omega = 1.00$ in the multi-objective problem. The other extreme when $\omega = 0.00$, is the trivial case of minimization of degradation, which takes place when the storage is not operated, leading to zero degradation and zero revenue.

5.2. Multi-objective optimization

A parametric sweep is carried out next, starting with $\omega = 0.95$ and decreasing it by 0.05 in every iteration. The results for the naive objective and the multi-objective approach are shown in Fig. 6. The naive objective which only maximizes revenue also maximizes the degradation in the battery. Results for thirteen values of ω are compared with this as a basis. As the weight is decreased, the revenue from the market decreases as well as the battery degradation. However, the proportions by which each objective decreases are not equal. Each point in Fig. 6 represents a Pareto optimal scheduling strategy. The algorithm finds intelligent scheduling strategies based on the input degradation data of the battery by modulating the charge and discharge states with time-based on the price signals. In order to understand better how the algorithm works, two such Pareto optimal scheduling strategies ($\omega = 0.8$ and $\omega = 0.4$) are compared against the base case in Fig. 7.

In the naive case, every opportunity to generate revenue from the market is fully utilized. This results in abrupt changes in SOC which causes high degradation in the storage system. When $\omega = 0.8$, the scheduling strategy is more biased towards revenue generation than preservation of the storage. Still, it can bring down the degradation by about 22.7% while generating 98.8% of the maximum revenue. This is made possible by only charging and discharging at the maximum current when the prices are either very low or very high, respectively. In other trading intervals, the current is reduced or cycling at high SOC is completely avoided (e.g., in $t_{40} - t_{45}$). The scheduling strategy when $\omega = 0.4$ gives much importance to the degradation in the battery. This is evident from Fig. 6, where degradation is only 23.7% of the maximum. However, 86.9% of the maximum revenue is still possible. The way the storage is operated in this scheduling strategy is to spread out the charging and discharging over longer intervals. Also, very high states of charge are discernibly avoided until price differences justify them. Even when 100% state of charge is reached, it is done in stages with low currents applied at high states of charge (e.g., in $t_{15} - t_{18}$ and $t_{31} - t_{35}$ in Fig. 7). This strategy is akin to the charging scheme currently adopted for electric vehicles and devices such as mobiles and laptops where batteries are charged at a faster rate until they reach a SOC of 80% followed by charging at a reduced current.

5.3. Accuracy of the proposed degradation model

The actual battery degradation behaviour is non-linear. It was cast as a MILP with the addition of piecewise linear segments and binary variables approximating the actual non-linear behaviour. Six segments were used to linearize the square function in (18). The accuracy of this MILP is compared against the non-linear post-optimization computation in Table 2. It can be noticed that the MILP represents the non-linear degradation behaviour with good accuracy.

The importance of including the current dependence can be gauged by calculating the degradation that would have been caused with the same scheduling strategy when no dependence of degradation on current is assumed. Thus, the degradation caused, for example, at 2C charge rate is the same as 1C discharge rate. Algorithmically, this is determined post-optimization by fixing the value of ψ to unity, which means that the value of d_t is always equal to d_t^{1C}. The error introduced by this assumption has also been quantified in Table 2.

The actual degradation can also be compared against the Ah throughput model, which assumes no influence of current rate and average state of charge on degradation. The degradation from this approach can be calculated post-optimization from the data available from the battery data sheet (Table 1). The degradation caused by one Ah of charge/discharge is equal to 120 μAh. The inadequacy of this approach to represent degradation for this battery is evident from the results presented in Table 2.

The aforementioned data indicate that a scheduling strategy for an energy storage system based on lithium-ion batteries that is derived using incorrect degradation models is likely to be far from the actual optimum.

5.4. Simulating a medium-term scheduling horizon – application of the decomposition technique

The application of the proposed two-stage temporal decomposition technique for solving the optimization problem for more trading intervals is demonstrated by considering the day-ahead market prices for one week, from 22 January 2018 to 29 January 2018 for the UK SEM [43], which corresponds to 336 time intervals. To make the problem even more difficult and highlight the utility of the proposed decomposition approach, $\omega = 0.3$ is used. For this value of ω, a solution with zero optimality gap could not be obtained even after 3600s for the 48 interval problem discussed in the previous sections.

When optimizing the 336-interval optimization problem as a whole, the composite objective function value ζ progress with time is as shown in Table 3. The incremental progress is very slow after 1500s. Using the two-stage decomposition approach, the optimization horizon is subdivided into 14 optimization periods of 24 intervals each. The intermediate SOC values are set using the best solution case at 1500s. Each sub-period is then individually optimized. The value of ζ after adding the individual sub-periods is found to be 116.89. The entire two-stage optimization routine runs in less than 2000s and outputs a better scheduling strategy than the original program even after 36000s. This strategy is illustrated in Fig. 5. In terms of the two objectives, this scheduling strategy yields 79% of the maximum revenue (€497.15 vs. €629.45) while reducing the degradation by 81.6% (4.61 mAh vs. 25.12 mAh). Degradation measured as capacity fade in one battery unit forming the storage system is also plotted in Fig. 8. Sharp changes of SOC at high SOC values cause the most capacity fade in the battery. There is a scope of further improvement in the total time taken by the optimization routine by solving the decoupled sub-problems in parallel rather than sequentially.

The effectiveness of the two-stage decomposition technique vs. the heuristic of fixing the intermediate SOC values to 50% can also be adjudged. To evaluate the dispatch strategy using the heuristic, only the second stage of the two-stage decomposition technique is run after fixing the intermediate states to the value of 50%. The 336-interval optimization problem yields the dispatch strategy which can be seen in Fig. 8. In this case, the value of the composite objective function is 104.92. The simulation takes less than 1200s. The value of the objective function is however considerably lower than the one obtained by the

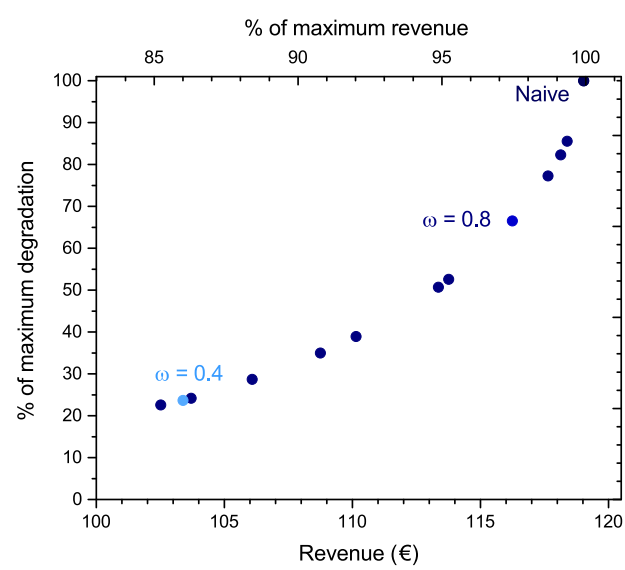

Fig. 6. Pareto efficient scheduling strategies for the day-ahead market.

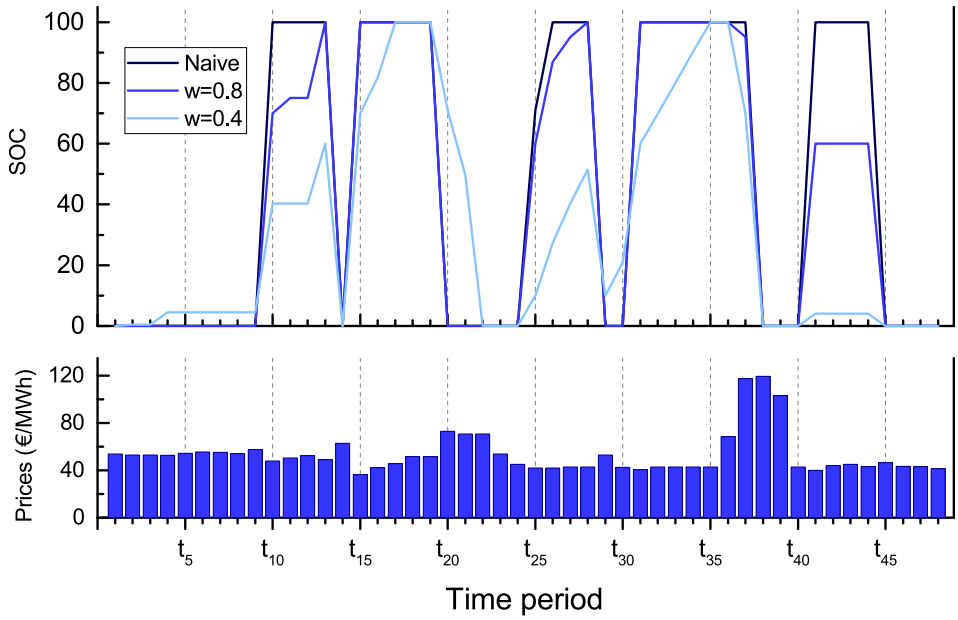

Fig. 7. Dispatch strategy for three cases. The naive case does not take battery degradation into account. The other two cases increasingly penalize degradation.

two-stage technique (116.89) demonstrating the effectiveness of this two-stage technique. In terms of the two objectives, revenues of €455.5 are generated and degradation of 4.53 mAh is caused for the case when $\omega = 0.3$ using the heuristic approach.

6. Conclusion

A more accurate way to quantify and account for non-linear degradation behaviour of lithium-ion batteries in storage scheduling models applied to power systems has been presented in this work. Even though the capacity fading model proposed is not totally reliable, it presents an efficient compromise between speed and accuracy based on experimental data collected from a battery with the same chemistry provided by the same manufacturer. A novel multi-objective approach to optimize for revenue while taking degradation in lithium-ion batteries into account has been proposed. Evidently, multiple Pareto optimal operating strategies for storage systems are possible, the selection of which will require decision making based not only on the capital and operating costs of these batteries but also the short-term and long-term financial goals of the energy storage system operator. The proposed mixed-integer linear programming based model is also applicable for more computationally intensive optimization studies through the two-stage temporal decomposition technique that was proposed. It is to be noted that although the proposed model is applicable to lithium batteries of different chemistries, the exact degradation parameters used in this work are applicable only to the NMC battery under study.

Table 3
Solution progress of the original 336-interval problem.

Time (s)	Value of ζ
1000	111.29
1500	113.69
3600	115.94
10000	116.25
15000	116.26
36000	116.36

Degradation parameters for other batteries can be determined based on aging experiments following the methodology in [34] or by using aging datasets that are openly available [44]. Once the degradation parameters are determined, the linearisation techniques proposed in this work can be used. The important revenue versus degradation trade-off highlighted in this work can be easily replicated for other batteries, provided that the experimental data on their degradation behaviour are available.

Declaration of Competing Interest

The authors declare that they have no known competing financial interests or personal relationships that could have appeared to influence the work reported in this paper.

Table 2
Comparison of errors using different optimization and degradation models.

Case	Non-linear	MILP (6 segment)		Current independent		Ah Throughput	
	Degradation (mAh)	Degradation (mAh)	% error	Degradation (mAh)	% error	Degradation (mAh)	% error
Naive	4.65	4.60	1.07	3.72	20.11	2.58	44.52
$\omega = 0.9$	3.99	3.94	1.26	4.77	−19.58	2.42	39.42
$\omega = 0.8$	3.56	3.56	0.13	3.89	−9.20	2.37	33.34
$\omega = 0.7$	2.45	2.42	1.38	3.29	−34.02	2.06	16.11
$\omega = 0.6$	1.81	1.79	1.18	2.18	−20.55	1.81	0.25
$\omega = 0.5$	1.34	1.32	1.08	2.40	−79.89	1.63	−21.94
$\omega = 0.4$	1.11	1.09	1.58	1.84	−66.43	1.58	−42.62

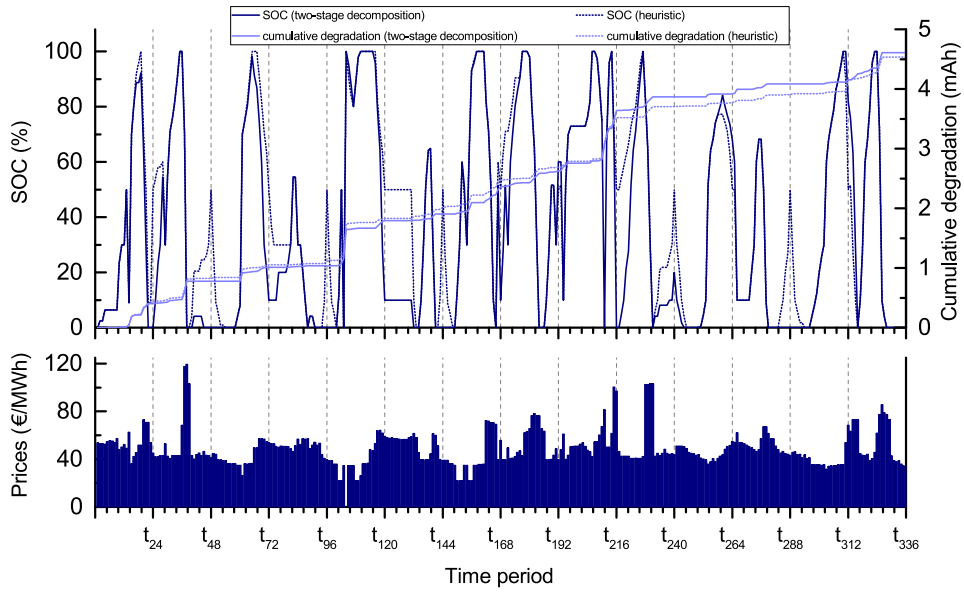

Fig. 8. Scheduling strategy for the week-long multi-objective optimization problem for $\omega = 0.3$ plotted along with electricity prices for the two-stage decomposition technique and the heuristic approach of fixing intermediate SOC at 50%.

References

[1] Gandoman FH, Jaguemont J, Goutam S, Gopalakrishnan R, Firouz Y, Kalogiannis T, et al. Concept of reliability and safety assessment of lithium-ion batteries in electric vehicles: basics, progress, and challenges. Appl Energy 2019;251:113343.

[2] Wang Y, Sun Z, Chen Z. Energy management strategy for battery/supercapacitor/fuel cell hybrid source vehicles based on finite state machine. Appl Energy 2019;254:113707.

[3] Zhang C, Wang Y, Gao Y, Wang F, Mu B, Zhang W. Accelerated fading recognition for lithium-ion batteries with Nickel-Cobalt-Manganese cathode using quantile regression method. Appl Energy 2019;256:113841.

[4] Zhu R, Duan B, Zhang C, Gong S. Accurate lithium-ion battery modeling with inverse repeat binary sequence for electric vehicle applications. Appl Energy 2019;251:113339.

[5] Wang Y, Li X, Wang L, Sun Z. Multiple-grained velocity prediction and energy management strategy for hybrid propulsion systems. J Energy Storage 2019;26:100950.

[6] Goebel C, Hesse H, Schimpe M, Jossen A, Jacobsen HA. Model-based dispatch strategies for lithium-ion battery energy storage applied to pay-as-bid markets for secondary reserve. IEEE Trans Power Syst 2017;32(4):2724–34.

[7] Fares RL, Webber ME. A flexible model for economic operational management of grid battery energy storage. Energy 2014;78:768–76.

[8] Pelzer D, Ciechanowicz D, Knoll A. Energy arbitrage through smart scheduling of battery energy storage considering battery degradation and electricity price forecasts. In: 2016 IEEE Innovative Smart Grid Technologies - Asia (ISGT-Asia), 2016, p. 472–7.

[9] Xu B, Zhao J, Zheng T, Litvinov E, Kirschen DS. Factoring the cycle aging cost of batteries participating in electricity markets. IEEE Trans Power Syst 2018;33(2):2248–59.

[10] Zhai Q, Meng K, Dong ZY, Ma J. Modeling and analysis of lithium battery operations in spot and frequency regulation service markets in Australia electricity market. IEEE Trans Industr Inf 2017;13(5):2576–86.

[11] Kazemi M, Zareipour H. Long-term scheduling of battery storage systems in energy and regulation markets considering battery's lifespan. IEEE Trans Smart Grid 2018;9(6):6840–9.

[12] He G, Chen Q, Kang C, Pinson P, Xia Q. Optimal bidding strategy of battery storage in power markets considering performance-based regulation and battery cycle life. IEEE Trans Smart Grid 2016;7(5):2359–67.

[13] Shafiee S, Zamani-Dehkordi P, Zareipour H, Knight AM. Economic assessment of a price-maker energy storage facility in the Alberta electricity market. Energy 2016;111:537–47.

[14] Wankmüller F, Thimmapuram PR, Gallagher KG, Botterud A. Impact of battery degradation on energy arbitrage revenue of grid-level energy storage. J Energy Storage 2017;10:56–66.

[15] Kazemi M, Zareipour H, Amjady N, Rosehart WD, Ehsan M. Operation scheduling of battery storage systems in joint energy and ancillary services markets. IEEE Trans Sustainable Energy 2017;8(4):1726–35.

[16] Akhavan-Hejazi H, Mohsenian-Rad H. Optimal operation of independent storage systems in energy and reserve markets with high wind penetration. IEEE Trans Smart Grid 2014;5(2):1088–97.

[17] Li Y, Vilathgamuwa M, Choi SS, Farrell TW, Tran NT, Teague J. Development of a degradation-conscious physics-based lithium-ion battery model for use in power system planning studies. Appl Energy 2019;248:512–25.

[18] Hoke A, Brissette A, Smith K, Pratt A, Maksimovic D. Accounting for lithium-ion battery degradation in electric vehicle charging optimization. IEEE J Emerg Sel Top Power Electron 2014;2(3):691–700.

[19] Dufo-López R, Bernal-Agustín JL, Domínguez-Navarro JA. Generation management using batteries in wind farms: economical and technical analysis for Spain. Energy Policy 2009;37(1):126–39.

[20] You S, Rasmussen CN. Generic modelling framework for economic analysis of battery systems. IET Conference on Renewable Power Generation (RPG 2011). 2011. p. 1–6.

[21] Teleke S, Baran ME, Bhattacharya S, Huang AQ. Optimal control of battery energy storage for wind farm dispatching. IEEE Trans Energy Convers 2010;25(3):787–94.

[22] Duggal I, Venkatesh B. Short-term scheduling of thermal generators and battery storage with depth of discharge-based cost model. IEEE Trans Power Syst 2015;30(4):2110–8.

[23] Tan X, Wu Y, Tsang DHK. A stochastic shortest path framework for quantifying the value and lifetime of battery energy storage under dynamic pricing. IEEE Trans Smart Grid 2017;8(2):769–78.

[24] Namor E, Torregrossa D, Sossan F, Cherkaoui R, Paolone M. Assessment of battery ageing and implementation of an ageing aware control strategy for a load leveling application of a lithium titanate battery energy storage system. 2016 IEEE 17th Workshop on Control and Modeling for Power Electronics (COMPEL). 2016. p. 1–6.

[25] Thaller L. Expected cycle life versus depth of discharge relationships of well behaved single cells and cell strings. In: 162nd Meeting of the Electrochem. Soc., Detroit, 17-22 Oct. 1982; 1982, p. 17–22.

[26] Bindner H, Cronin T, Lundsager P, Manwell JF, Abdulwahid U, Baring-gould I. Lifetime modelling of lead acid batteries, vol. 1515, 2005. http://130.226.56.153/rispubl/VEA/veapdf/ris-r-1515.pdf.

[27] Schiffer J, Sauer DU, Bindner H, Cronin T, Lundsager P, Kaiser R. Model prediction for ranking lead-acid batteries according to expected lifetime in renewable energy systems and autonomous power-supply systems. J Power Sources 2007;168(1):66–78. 10th European lead battery conference.

[28] Castelo-Becerra A, Zeng W, Chow M. Cooperative distributed aggregation algorithm for demand response using distributed energy storage devices. North American Power Symposium (NAPS), 2017. 2017. p. 1–6.

[29] Ahmadian A, Sedghi M, Mohammadi-ivatloo B, Elkamel A, Aliakbar Golkar M, Fowler M. Cost-benefit analysis of V2G implementation in distribution networks considering PEVs battery degradation. IEEE Trans Sustainable Energy 2018;9(2):961–70.

[30] Fortenbacher P, Mathieu JL, Andersson G. Modeling, identification, and optimal control of batteries for power system applications. 2014 Power systems computation conference. 2014. p. 1–7.

[31] Zakeri B, Syri S. Value of energy storage in the Nordic Power market - benefits from price arbitrage and ancillary services. 2016 13th International Conference on the European Energy Market (EEM). 2016. p. 1–5.

[32] Tang X, Zou C, Yao K, Lu J, Xi Y, Gao F. Aging trajectory prediction for lithium-ion batteries via model migration and bayesian monte carlo method. Appl Energy 2019;254:113591.

[33] Schmitt J, Maheshwari A, Heck M, Lux S, Vetter M. Impedance change and capacity fade of lithium nickel manganese cobalt oxide-based batteries during calendar aging. J Power Sources 2017;353:183–94.

[34] Maheshwari A, Heck M, Santarelli M. Cycle aging studies of lithium nickel manganese cobalt oxide-based batteries using electrochemical impedance spectroscopy. Electrochim Acta 2018;273:335–48.

[35] Ecker M, Nieto N, Käbitz S, Schmalstieg J, Blanke H, Warnecke A, Sauer DU.

Calendar and cycle life study of Li(NiMnCo)O2-based 18650 lithium-ion batteries. J Power Sources 2014;248:839–51.
[36] Schmalstieg J, Käbitz S, Ecker M, Sauer DU. A holistic aging model for Li(NiMnCo)O2 based 18650 lithium-ion batteries. J Power Sources 2014;257:325–34.
[37] Lewerenz M, Sauer DU. Evaluation of cyclic aging tests of prismatic automotive LiNiMnCoO2-graphite cells considering influence of homogeneity and anode overhang. J Energy Storage 2018;18:421–34.
[38] Laresgoiti I, Käbitz S, Ecker M, Sauer DU. Modeling mechanical degradation in lithium ion batteries during cycling: Solid electrolyte interphase fracture. J Power Sources 2015;300:112–22.
[39] Paterakis NG, Gibescu M, Kout W, Hugo YA. Investigation of arbitrage between the Dutch day-ahead and imbalance markets as a business case for the hydrogen bromine flow battery. 2017 IEEE Manchester PowerTech. 2017. p. 1–6.
[40] Padberg M. Approximating separable nonlinear functions via mixed zero-one programs. Operat Res Lett 2000;27(1):1–5.
[41] Keha AB, de Farias IR, Nemhauser GL. Models for representing piecewise linear cost functions. Operat Res Lett 2004;32(1):44–8.
[42] Kim K, Botterud A, Qiu F. Temporal decomposition for improved unit commitment in power system production cost modeling. IEEE Trans Power Syst 2018;33(5):5276–87.
[43] ENTSO-E Transparency Platform, https://transparency.entsoe.eu/, accessed 2018-04-22.
[44] CALCE Battery Research Group Data, https://web.calce.umd.edu/batteries/data.htm, accessed 2019-11-24.